Discovery of Potent Antagonists of the Antiapoptotic Protein XIAP for the Treatment of Cancer

Thorsten K. Oost,*,† Chaohong Sun,† Robert C. Armstrong,‡ Ali-Samer Al-Assaad,‡ Stephen F. Betz,§ Thomas L. Deckwerth,‡ Hong Ding,† Steven W. Elmore,† Robert P. Meadows,# Edward T. Olejniczak,† Andrew Oleksijew,† Tilman Oltersdorf,‡ Saul H. Rosenberg,† Alexander R. Shoemaker,† Kevin J. Tomaselli,‡ Hua Zou,‡ and Stephen W. Fesik*,†

Cancer Research, Global Pharmaceutical Research and Development, Abbott Laboratories, 100 Abbott Park Road, Abbott Park, Illinois 60064, Idun Pharmaceuticals, 9380 Judicial Drive, San Diego, California 92121, Neurocrine Biosciences, 10555 Science Center Drive, San Diego, California 92121, and Ferring Research Institute, 3550 General Atomics Court, San Diego, California 92121

Received February 13, 2004

Inhibitor of apoptosis (IAP) proteins are overexpressed in many cancers and have been implicated in tumor growth, pathogenesis, and resistance to chemo- or radiotherapy. On the basis of the NMR structure of a SMAC peptide complexed with the BIR3 domain of X-linked IAP (XIAP), a novel series of XIAP antagonists was discovered. The most potent compounds in this series bind to the baculovirus IAP repeat 3 (BIR3) domain of XIAP with single-digit nanomolar affinity and promote cell death in several human cancer cell lines. In a MDA-MB-231 breast cancer mouse xenograft model, these XIAP antagonists inhibited the growth of tumors. Close structural analogues that showed only weak binding to the XIAP−BIR3 domain were inactive in the cellular assays and showed only marginal in vivo activity. Our results are consistent with a mechanism in which ligands for the BIR3 domain of XIAP induce apoptosis by freeing up caspases. The present study validates the BIR3 domain of XIAP as a target and supports the use of small molecule XIAP antagonists as a potential therapy for cancers that overexpress XIAP.

Introduction

Apoptosis plays a critical role in the development and homeostasis of multicellular organisms. Inappropriate suppression or activation of apoptosis can lead to a variety of diseases. For example, in many cancers the cell death machinery is inhibited by the upregulation of antiapoptotic proteins, suggesting that the restoration of apoptotic activity might be an effective approach for treating these cancers. Members of the inhibitor of apoptosis (IAP) family of proteins are upregulated in cancers[1−3] and inhibit programmed cell death through their ability to directly inhibit members of the caspase family of apoptotic enzymes. Human X-linked IAP (XIAP), the best-characterized among the IAPs, is believed to directly inhibit particular caspases via its ∼70-amino acid baculovirus IAP repeat (BIR) domains. The BIR3 domain of XIAP binds directly to the small subunit of caspase-9,[1,4] the initiator caspase in the mitochondrial pathway of apoptosis. As evident from the X-ray structure of the complex, XIAP sequesters caspase-9 in a catalytically inactive monomeric state, thus preventing formation of the catalytically active caspase-9 homodimer.[5] On the other hand, a region containing the BIR2 domain of XIAP inhibits the executioner caspases 3 and 7,[6−8] which prevents normal substrate processing and leads to the inhibition of apoptosis. Recently, a mammalian protein called SMAC (also called DIABLO) was identified that triggers apoptosis by abrogating the inhibitory effects of IAPs on caspases.[9,10] SMAC promotes caspase-9 activation by competing with the caspase for the same binding groove on the surface of the BIR3 domain. The structural basis for the binding of SMAC to the BIR3 domain of XIAP has been elucidated by NMR and X-ray structural analysis.[11−13] The SMAC N-terminus binds to the BIR3 domain in an extended conformation with only the first four amino acid residues (AVPI) contacting the protein. This tetrapeptide motif was envisioned as a good starting point for the design of peptidomimetic compounds that would bind to XIAP and induce apoptosis in a fashion similar to the protein SMAC. Such SMAC mimetics may be useful for treating cancers that are resistant to proapoptotic drugs due to the overexpression of IAPs. Indeed, several groups have reported that SMAC-derived peptides that bind to XIAP can sensitize cancer cell lines to undergo programmed cell death.[14−16] Peptides have also been shown to have an effect in an in vivo intracranial malignant glioma xenograft model.[17] A peptide comprised of the 7mer N-terminus of SMAC linked to the shuttle peptide TAT from HIV strongly enhanced the antitumor activity of Apo2L/TRAIL in this in vivo model. Despite these impressive studies, the use of a peptide from the SMAC N-terminus as a therapeutic agent has several disadvantages. First, truncated N-terminal SMAC peptides bind only weakly to the BIR3 domain of XIAP ($K_d \sim 0.5\ \mu M$).[11] Furthermore,

* Address correspondence to either author: Thorsten K. Oost, Abbott GmbH & Co. KG, Knollstrasse, 67061 Ludwigshafen, Germany; ph: +49 (0)621 589 2141; e-mail: thorsten.oost@abbott.com; Stephen W. Fesik, Department 460, Bldg. AP10-LL, 100 Abbott Park Road, Abbott Park, IL 60064-6098, USA; ph: 847 937 1207; e-mail: stephen.fesik@abbott.com.

† Abbott Laboratories.
‡ Idun Pharmaceuticals.
§ Neurocrine Biosciences.
# Ferring Research Inst.

10.1021/jm040037k CCC: $27.50
Published on Web 07/31/2004

Table 1. Binding Affinity to the BIR3 Domain of XIAP for Representative Examples from the Peptide Libaries[a]

position 1	K_d [μM]	position 2	K_d [μM]	position 3	K_d [μM]	position 4	K_d [μM]
Ala	0.06	Val	0.06	Pro	0.06	Phe	0.06
Gly	9.6	Gly	2.7	Gly	3	Gly	3.4
Abu	0.04	Ala	0.29	Aib	>20	Val	0.9
Val	0.9	Abu	0.09	Sar	0.6	Leu	0.28
Nle	>20	Leu	0.16	Me-Ala	1.6	Ile	0.36
D-Ala	5	Nle	0.12	Hyp	0.8	Nle	0.9
Aib	1.8	Lys	0.05	Pip	0.4	Cha	0.97
Me-Ala	0.04	Phe	0.12	Aze	0.12	Tyr	0.3
Me_2-Ala	8.7	Tle	0.04			Cl-Phe	0.18
		D-Ala	>20			1-Nal	0.09
		D-Val	>20			2-Nal	0.19
		D-Phe	>20			Phg	0.03
		Aib	>20			homo-Phe	0.18
		Me-Ala	>20			D-Phe	0.8
						Aib	6.7

[a] All analogues were derived from the pentapeptide AVPFY. Four libraries were synthesized in which each of the first four residues was varied while keeping the other four residues unchanged. Abbreviations: α-aminobutyric acid (Abu), α-aminoisobutyric acid (Aib), azetidine-2-carboxylic acid (Aze), cyclohexylalanine (Cha), 4-chlorophenylalanine (Cl-Phe), (4*R*)-4-hydroxyproline (Hyp), 1-naphthylalanine (1-Nal), 2-naphthylalanine (2-Nal), norleucine (Nle), phenylglycine (Phg), pipecolic acid (Pip), sarcosine (Sar), *tert*-leucine (Tle). Unless indicated otherwise, amino acids have the L-configuration.

the therapeutic application of peptides is hampered in many cases by their proteolytic instability, limited cellular penetration, and poor pharmacokinetics.

Our goal was to improve the potency and proteolytic stability of the SMAC peptides to provide a compound that could be used to evaluate XIAP as a target for cancer chemotherapy in vitro and in vivo. In the present study, we report on the discovery of a series of proteolytically stable, capped tripeptides comprised of unnatural amino acids that bind to the BIR3 domain of XIAP with single-digit nanomolar affinity, display cytotoxic effects in cancer cell lines, and slow the growth of tumors in a MDA-MB-231 breast cancer mouse xenograft model.

Results and Discussion

SAR from Peptide Libraries. To rapidly determine the structure/activity relationships (SAR) for the binding of the individual residues of the SMAC N-terminal tetrapeptide, peptide libraries were synthesized employing high-throughput solid-phase peptide synthesis. We have previously shown that the N-terminus of processed HID, a functional homologue of SMAC found in lower organisms,[18] has a 4-fold higher binding affinity for the BIR3 domain of XIAP when compared to the corresponding SMAC peptide.[11] Therefore, as a starting point, it was decided to use AVPFY, the pentapeptide N-terminus of processed HID, that binds to the XIAP−BIR3 domain with an affinity of 60 nM. Four libraries were prepared in which each of the first four residues was varied while keeping the other four residues unchanged. A total of more than 120 compounds was synthesized and evaluated for binding to the BIR3 domain of XIAP by employing a fluorescent polarization assay.[11] Table 1 provides a summary of the BIR3 binding affinities for a representative group of peptides from these libraries. For position 1, only small residues with the natural L-configuration (e.g., Ala or Abu) are accommodated, which is in good agreement with the three-dimensional structure of the SMAC/XIAP−BIR3 complex in which the Ala methyl group fits tightly into the protein pocket.[11] The importance of the hydrophobic interaction between the Ala methyl group and W310 of BIR3 is underscored by the lack of activity for the Gly analogue. Substitution of the terminal amino group with one methyl group was found to be tolerated without loss of binding affinity. However, *N*,*N*-dimethyl substitution abolishes binding. The peptide library in which position 2 was varied afforded a relatively shallow SAR profile (K_d values between 0.04 and 0.29 μM) for L-configured neutral and basic residues, concordant with the side chain of residue 2 pointing away from the protein into solution. Residues with a D-configuration or those containing a *gem*-dimethyl motif (Aib) were inactive. These results are consistent with the 3D structure of the SMAC/XIAP−BIR3 complex in which the side chain of a D-amino acid is predicted to clash sterically with the protein. The relatively weak binding affinity of the Gly analogue may be caused by a lack of conformational rigidity, as compared with analogues that bear L-configured residues in the second position. Replacing the Val at position 2 with *N*-Me-Ala abolished binding to the BIR3 domain, underscoring the importance of the intermolecular hydrogen bond involving the amide of residue 2 which stabilizes complex formation. Attempts to replace Pro in position 3 with a variety of amino acids, in most cases, resulted in a significant loss of binding affinity. In the SMAC/XIAP−BIR3 complex the 4 (gamma) and 5 (delta) methylene groups of the proline ring contact Trp 323. The contacts with the 5 (delta) position of the proline ring cannot be mimicked by other natural amino acids. In addition, a proline at this position may conformationally restrict the peptide. Interestingly, the azetidine (Aze) analogue bearing a four- instead of a five-membered ring afforded a similar binding affinity as the Pro analogue, suggesting a closely related bioactive conformation. In position 4, aromatic residues, such as Phg, Phe, homo-Phe (in this order), or 1-naphthylalanine (1-Nal), afforded the best binding affinities. It is interesting to note, however, that aliphatic residues of comparable hydrophobicity, such as cyclohexylalanine (Cha), exhibited over a 10-fold loss of binding affinity. This result is consistent with previous findings[19] as well as with the fact that other BIR3 binding proteins, such as Reaper, Hid, Sickle and human caspase-9 carry an aromatic residue in the corresponding position. NMR studies on a AVPF/XIAP−BIR3 peptide complex were consistent with a binding mode that is similar to the SMAC-derived tetrapeptide AVPI. In particular, NOEs from the Phe of the AVPF peptide and Gly 306, Lys 297, and Lys 299 indicated that the Phe of the peptide sat in the same pocket as the parent Ile. These data support the hypothesis that the preference for Phe is due to the additional favorable hydrophobic interactions that arise from placing a phenyl ring between the hydrophobic portion of the side chains of Lys 297 and Lys 299 (Figure 1A).

SAR from Capped Tripeptide Libraries. To reduce the peptide character of the pentapeptide lead and improve the binding affinity, a series of more than 150 capped tripeptides was designed and synthesized in a high-throughput parallel format (Scheme 1). Assembly

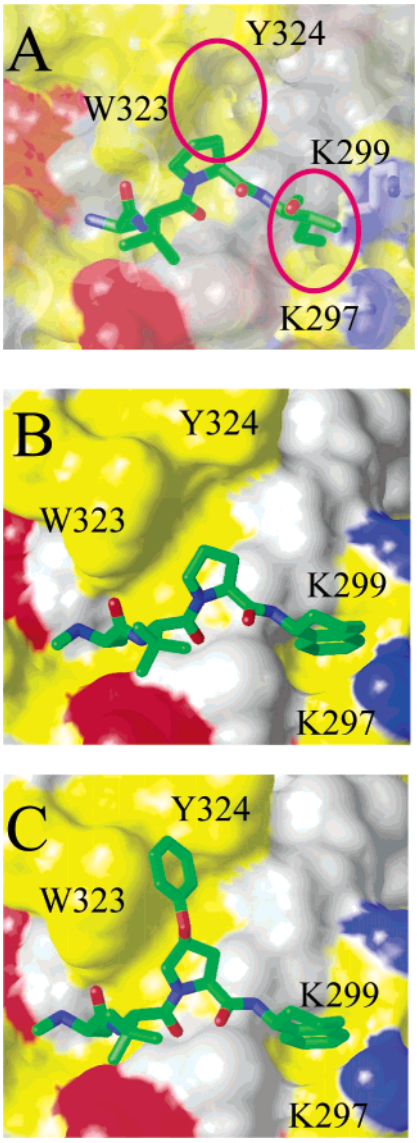

Figure 1. (A) A transparent solvent-accessible surface showing the AVPI terminus of the SMAC peptide bound to the BIR3 domain of XIAP[11] (PDB ID: 1G3F). Two potential sites for improving the binding affinity of the tetrapeptide lead are indicated by red ovals. (B) Solvent-accessible surface showing compound **2** bound to the BIR3 domain of XIAP (PDB ID: 1TFQ). (C) Compound **10** bound to the BIR3 domain of XIAP (PDB ID: 1TFT). Leu, Ile, Val, Met, Tyr, Phe, Trp, and the hydrophobic side chain of Lys are colored yellow. Asp and Glu are colored red. Arg, His and the amino group of Lys are colored blue. All other residue types are colored gray. The side chains for Lys 297, Lys 299, Trp 323, and Tyr 324 are shown.

of the benzyl protected tripeptide Boc-AVP-OBn was conducted using standard peptide coupling conditions. After hydrogenolytic cleavage of the benzyl ester, the resulting acid Boc-AVP-OH was coupled to a variety of amines employing solid-phase reagents. Epimerization is of no concern in this coupling reaction, since the carboxylic acid function is part of a proline residue, and, thus, oxazolone formation is impossible. Given the observed preference for aromatic residues in position 4, mostly amines comprising an aromatic or heteroaromatic ring were selected for C-terminal capping. The final products were obtained after removal of the Boc protecting group and preparative HPLC purification. The BIR3 binding data observed for this first library is enclosed in the Supporting Information. Analogues bearing phenyl-alkyl amide caps with linear alkyl spacers and optional ring substitutions showed only moderate to weak binding to the BIR3 protein. However, binding increased to ≤50 nM levels with benzyl amide caps that are branched in the benzylic position, with the tetrahydronaphthyl amide being the most active cap in the first round. From the SAR of the peptide libraries (Table 1), it was concluded that Ala in position 1 and Val in position 2 can be replaced with *N*-Me-Ala and Tle (*tert*-leucine), respectively, without loss of binding affinity. Combination of these unnatural amino acid residues with the most promising amide caps discovered in the first library led to the development of a second library. The binding affinities of representative examples from this library are presented in Table 2. Conformational restriction of the aromatic ring in the (*R*)-tetrahydronaphthyl amide analogue **2** and (*R*)-indane amide analogue **4** resulted in potent ligands of XIAP−BIR3 (K_d = 0.012 and 0.029 μM, respectively). The diastereomer analogues **3** and **5** showed markedly reduced binding affinities, suggesting that only the (*R*)-configuration places the aromatic ring in a favorable position for binding. A model of compound **2** docked into the BIR3 domain of XIAP indicated that the (*R*)-configuration of the tetrahydronaphthyl amide cap corresponds to the L-configuration of position 4 amino acids. Thus, the (*R*)-tetrahydronaphthyl and indane amide groups can be regarded as conformationally restricted versions of L-Phg, which is the amino acid that afforded the best binding affinity in this position (Table 1). The structure of compound **2** bound to XIAP−BIR3 was determined and is shown in Figure 1B. The structure confirms that only the (*R*)-configuration provides a vector that places the tetrahydronaphthyl group in the correct geometry for interaction with the hydrophobic alkyl portions of Lys 297 and Lys 299. This substitution causes the proline at position 3 and the phenyl ring of the tetrahydronaphthyl at position 4 to fill more of the pocket than the corresponding Pro and Ile residues of the original SMAC tetrapeptide (Figure 1A). This change is supported by NOE contacts between Leu 292 and the tetrahydronaphthyl at position 4, which were not observed for the Ile at position 4 in the SMAC tetrapeptide complex.[11] Attachment of achiral 1- and 2-naphthyl amide caps (sp^2 connection) resulted in the inactive analogues **6** and **7**. In contrast, the less planar fluorenyl amide analogue **8** (sp^3 connection) was well-tolerated, underscoring the subtle conformational preferences for this position. Overall, optimization of the cap portion resulted in compounds **2** and **4** with low double-digit nanomolar binding affinity for the XIAP−BIR3 domain. Importantly, compound **2** was shown to be stable in plasma and mouse whole blood (2 h incubation at 37 °C) and during the time needed to conduct the cell-based experiments (data not shown).

To further enhance the binding affinity of the peptidomimetic BIR3 ligands, additional sites not accessed by the original peptides were pursued. From an analysis of the structure of the SMAC/XIAP−BIR3 complex it appeared that an additional hydrophobic groove made up by W323 and Y324 (Figure 1A) could be accessed by modification of the 4-position of the Pro residue. Particularly, the tetrahydronaphthyl cap in compound **2**

Scheme 1. Synthesis of Capped Tripeptide Libraries[a]

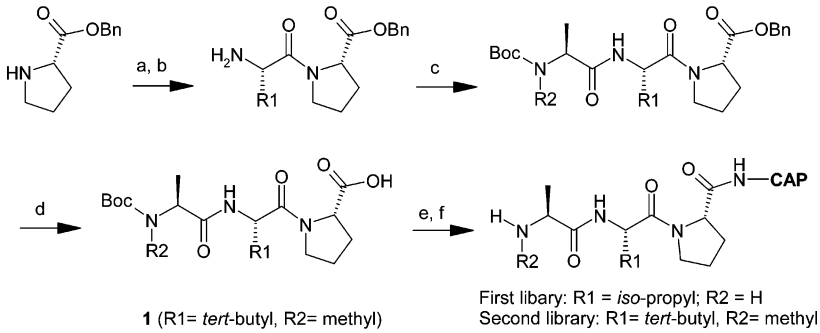

[a] Reagents and conditions: (a) Boc-Val-OH or Boc-Tle-OH, EDCI, HOBt, DIPEA, DMF; (b) 4 N HCl in dioxane; (c) Boc-Ala-OH or Boc-*N*-Me-Ala-OH, EDCI, HOBt, DIPEA, DMF; (d) H_2, Pd on carbon, MeOH; (e) Cap-NH_2, PS-Carbodiimide resin, HOAt, PS-Trisamine resin, DMA/DCE 1:1; (f) TFA/H_2O/TIS (95:2.5:2.5).

Table 2. Binding Affinity to the XIAP−BIR3 Domain for Representative Examples from the Second Library of Capped Tripeptides

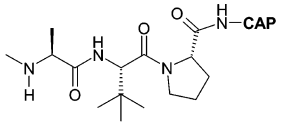

Compound	CAP	BIR3 K_d [μM] [a]
2	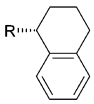	0.012
3	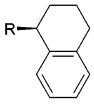	0.706
4	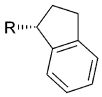	0.029
5	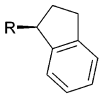	> 1
6	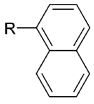	> 0.5
7	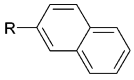	> 1
8	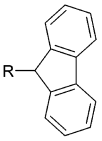	0.047
9	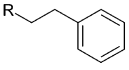	0.167

[a] Values are representative of at least two measurements.

causes a slight change in the Pro position and improves the vector from the Pro 4-position into this pocket (Figure 1B). Several capped tripeptides that bear hydrophobic substituents in the 4-position of Pro were prepared as outlined in Scheme 2 by employing standard peptide coupling protocols. In fact, compounds **10** and **12** comprising a (4*S*)-4-phenoxy-Pro residue in position 3 (*tert*-leucine and cyclohexylglycine in position 2, respectively) showed an almost 3-fold improved binding affinity compared to the unsubstituted analogues **2** and **11** (Table 3). A structure of compound **10** complexed to XIAP−BIR3 is shown in Figure 1C. This compound binds to BIR3 in a manner similar to compound **2** (Figure 1B) and the SMAC peptide (Figure 1A). The phenoxy substituent at the Pro 4-position leans against Trp 323 of BIR3, and stacking of the aromatic rings may contribute favorably to compound binding. Compounds **10** and **12** that are comprised solely of unnatural amino acid residues afforded single-digit nanomolar binding affinity for the BIR3 domain of XIAP.

Proapoptotic Activity of XIAP−BIR3 Ligands in Reconstituted Assays. To evaluate the ability of the BIR3 ligands to mimic the proapoptotic protein SMAC by relieving the inhibition of caspases by XIAP, selected analogues were tested in an in vitro assay system described previously.[21] In the fully reconstituted assay containing Apaf-1, caspase-9 (p35/p12), procaspase-3, dATP and cytochrome *c*, the potent BIR3 ligands **2**, **10**, and **11** (K_d = 0.005−0.016 μM) were found to rescue BIR3-mediated inhibition of caspase activity at submicromolar levels (Table 4). Compound **9** (phenethyl amide cap) as well as full-length SMAC afforded micromolar EC_{50} values, which is in line with their diminished BIR3 binding affinity (K_d = 0.17 and 0.42 μM, respectively). However, in a reconstituted assay inhibited by full-length XIAP instead of BIR3, the activity of recombinant SMAC increased dramatically, by more than 2 orders of magnitude; in contrast, the activity of the BIR3 ligands **2**, **10**, and **11** was virtually unchanged. These findings suggest that the SMAC−XIAP interaction is not solely mediated through the BIR3 interface, and give support to a model in which SMAC interacts with XIAP as a dimer, likely involving interactions with other domains of XIAP, such as BIR2. Not surprisingly, these additional binding interactions cannot be mimicked by small molecules that were optimized solely for binding to the BIR3 domain of XIAP. Our findings are consistent with recent results which show that simultaneous interaction with both BIR2 and BIR3 domains are required for the relief of XIAP-mediated caspase inhibition by SMAC and suggest a 2:1 SMAC/XIAP interaction stoichiometry.[22] The *N*,*N*-dimethyl-Ala analogue **14**, which does not bind to the XIAP−BIR3 domain (Table 3), was inactive in the reconstituted assays. Thus, within the capped tripeptide series, the results of the reconstituted assay correlate with the direct measurement of binding to the BIR3 domain.

Scheme 2. Synthesis of Prosubstituted Capped Tripeptides[a]

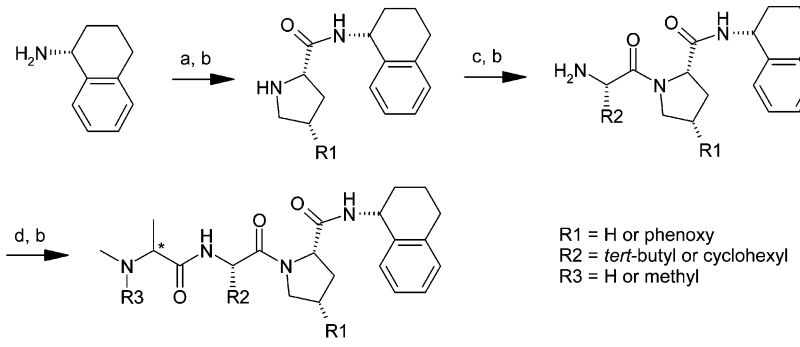

[a] Reagents and conditions: (a) Boc-Pro-OH or (4*S*)-Boc-4-phenoxy-Pro-OH, EDCI, HOBt, DIPEA, DMF; (b) 4 N HCl in dioxane; (c) Boc-Tle-OH or Boc-Chg-OH, EDCI, HOBt, DIPEA, DMF; (d) Boc-*N*-Me-Ala-OH or *N*,*N*-Me_2-Ala-OH or Boc-*N*-Me-D-Ala-OH, EDCI, HOBt, DIPEA, DMF. (4*S*)-Boc-4-phenoxy-Pro-OH was synthesized from commercially available Boc-Hyp-OMe in two steps.[20]

Table 3. Binding Affinity to the XIAP−BIR3 Domain of Pro- and Ala-Modified Capped Tripeptides

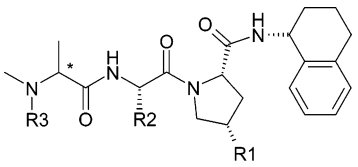

compound	R1	R2	R3	Ala configuration	BIR3 K_d[μM] [a]
2	H	*tert*-butyl	H	L	0.012
10	phenoxy	*tert*-butyl	H	L	0.005
11	H	cyclohexyl	H	L	0.016
12	phenoxy	cyclohexyl	H	L	0.006
13	H	*tert*-butyl	Me	L	>1
14	phenoxy	*tert*-butyl	Me	L	>1
15	H	cyclohexyl	Me	L	>1
16	H	*tert*-butyl	H	D	>1

[a] Values are representative of at least two measurements.

Table 4. Relief of Caspase Inhibition by BIR3 Ligands in Reconstituted Assays[a]

compound	BIR3 + APAF-1 + casp9 + procasp3 EC_{50} [μM][b]	XIAP + APAF-1 + procasp9 + procasp3 EC_{50} [μM][b]	BIR3 K_d [μM]
2	0.29	0.49	0.012
10	0.24	0.71	0.005
11	0.31	0.47	0.016
14	>100	>100	>1
9	1.26	4.21	0.167
SMAC	2.08	0.01	0.42

[a] Activity is expressed as an EC_{50}, the concentration at which half-maximum recovery was achieved. [b] Values are representative of at least two observations.

Cytotoxic Activity of XIAP−BIR3 Ligands in Human Cancer Cell Lines. To determine whether the proapoptotic activity that was observed in the reconstituted assays translates into cellular activity, the cytotoxicity of selected BIR3 ligands was assessed against various cancer cell lines (Table 5). Compounds **2** and **11** show a wide range of potencies against a panel of 59 human cancer cell lines ranging from single-digit nanomolar activity in some cell lines to no activity at 50 μM in most others. Both compounds exhibited similar activities in the cell lines in which they were examined, with compound **11** being slightly more potent than compound **2**. The highest potency was observed against the human breast cancer cell lines BT-549 and MDA-MB-231, the melanoma cell line SK-MEL-5, and the acute promyelocytic leukemia HL-60. There was no correlation between potency of compounds **2** and **11** and expression of XIAP,[2] suggesting that other factors contribute to sensitivity of the various cell lines. A sample dose−response curve of killing of MDA-MB-231 cells is shown in Figure 2A. The toxicity exhibited by the peptidomimetic BIR3 ligands in the sensitive cell lines occurs in the absence of an identified apoptotic stimulus. This observation is distinct from previous reports in which peptides with lower binding affinity for XIAP potentiated the toxicity of chemotherapeutic agents[14−16] or death receptor agonists.[15,17] To examine if BIR3 binding correlated with toxicity in cancer cell lines, negative control compounds with close structural similarity to the active analogues **2** and **11** were synthesized based on the SAR derived from the peptide libraries (Tables 1 and 2). Negative control compound **15** contains a *N*,*N*-dimethyl-Ala terminus, compound **16** is comprised of a *N*-methyl-D-Ala terminus, and compound **3** bears a mismatch C-terminal cap ((*S*)-tetrahydronaphthyl). In all cases, the weak BIR3 binding of these negative controls (Table 3) correlated well with strongly diminished cellular toxicity, consistent with the hypothesis that the active analogues kill susceptible human cancer cell lines in a mechanism-specific manner.

Inhibition of IAPs by SMAC induces caspase-dependent apoptosis.[9] Thus, it was predicted that the BIR3 ligands would induce caspase-3 activity in cells, and that caspase inhibition would promote cell survival. The susceptible mammary gland adenocarcinoma MDA-MB-231 cell line was exposed to either 1 μM or 10 nM concentrations of compound **11** for up to 30 h and caspase-3 activity was measured in cell lysates using DEVD-amc as a substrate. An up to 8-fold increase in caspase-3 activity was observed in a dose-dependent manner at 12−18 h following compound exposure (Figure 3). Exposure to 1 μM of the negative control **15** (*N*,*N*-dimethyl-Ala analogue) resulted in caspase-3 activity comparable to that of the suboptimal killing concentration of 10 nM of compound **11**. Incubation of compound **11**-treated cells with 10 μM of the pan-caspase inhibitor IDN-5370[23] reduced caspase-3 activity to the background level seen in untreated cells (Figure 3). Caspase inhibitor treatment completely protected MDA-MB-231 cells from an otherwise lethal concentration of compound **11** (Figure 2B) with an EC_{50} of 1 μM,

Table 5. Toxicity of BIR3 Ligands against the Eight Most Sensitive Human Cancer Cell Lines[a]

cell line	tissue type	exposure time (h)	2	3	16	11	15
BT-549	breast	72	0.015 ± 0.011 (4)	n.a.[b]	n.a.	0.007 ± 0.00035 (2)	1 ± 0.47 (4)
MDA-MB-231	breast	48	0.068 ± 0.031 (10)	3 ± 0.14 (2)	8.3 ± 1.8 (2)	0.013 ± 0.0056 (10)	3.4 ± 1.1 (8)
HL-60	leukemia	72	0.99 ± 1 (2)	n.a.	n.a.	0.19 ± 0.13 (2)	4.3 ± 3.1 (2)
SK-MEL-5	melanoma	48	1.3 ± 0.86 (4)	n.a.	n.a.	0.29 ± 0.22 (4)	15 ± 6.6 (4)
RXF-393	renal	72	0.81 ± 0.25 (2)	n.a.	n.a.	1.1 ± 0.14 (2)	>50 (2)
SK-OV-3	ovarian	48	1.5 ± 1.2 (6)	5.6 ± 0.42 (2)	>50 (2)	1.3 ± 1.1 (6)	>25 (4)
NCI-H23	NSCL	72	5.3 ± 2.1 (4)	n.a.	n.a.	1.5 ± 0.46 (4)	>50 (4)
NCI-H522	NSCL	72	1.7 ± 0.14 (2)	n.a.	n.a.	2 ± 0.64 (2)	>50 (2)

[a] An additional 52 cell lines tested showed less sensitivity to compound **11** and are listed in the Supporting Information. Compounds **3** and **16** are closely related in structure to compound **2**, but substantially less potent BIR3 ligands (Tables 2 and 3). Similarly, compound **15** is closely related to compound **11**. Cell lines were exposed to the compounds for 48 or 72 h in the presence of 10% FBS and viability was measured by MTS reduction. Mean EC_{50} [μM] ± SD (n). [b] n.a., not available.

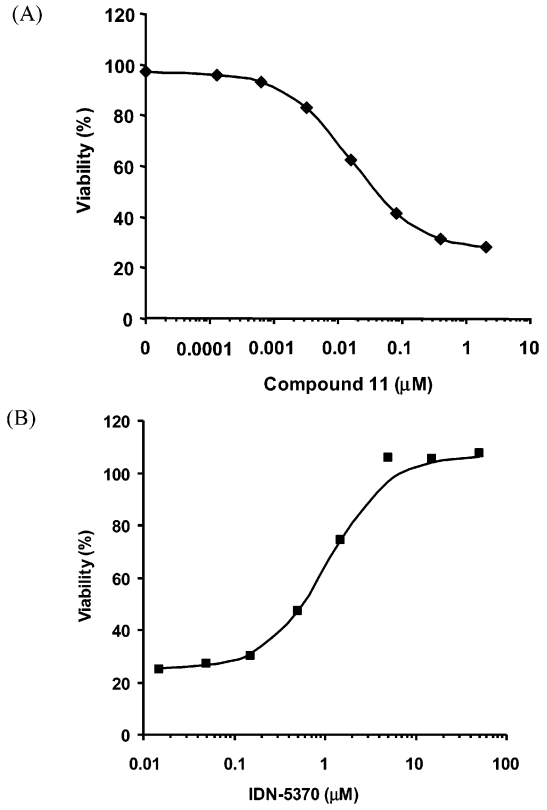

Figure 2. (A) Dose response curves of killing of MDA-MB-231 cells by compound **11**. MDA-MB-231 cells were cultured in 96-well plates for 48 h in the presence of various concentrations of compound **11** and viability was measured. (B) Promotion of survival of compound **11**-exposed MDA-MB-231 cells by the pan-caspase inhibitor IDN-5370. MDA-MB-231 cells were exposed to 10 μM of compound **11** and variable concentrations of the pan-caspase inhibitors IDN-5370 for 48 h, followed by measuring viability.

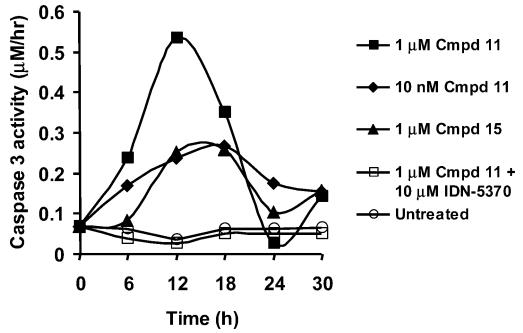

Figure 3. Time course of caspase-3 activity in cell lysates of MDA-MB-231 cells exposed to compounds **11** and **15** and the broad-spectrum caspase inhibitor IDN-5370. Maximum caspase-3 activity was observed at 12−18 h after addition of 10 nM to 1 μM of the BIR3 potent ligand **11**. Exposure of the cells to 10 μM of IDN-5370 during the time of incubation with 1 μM of compound **11** inhibited caspase-3 quantitatively.

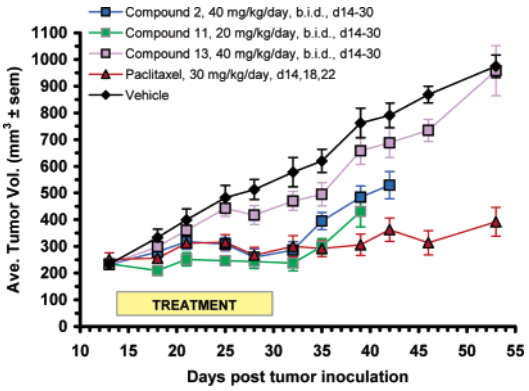

Figure 4. Comparison of efficacy of compound **2** (40 mg/kg/day, sc), compound **11** (20 mg/kg/day, sc), and negative control **13** (40 mg/kg/day, sc) to paclitaxel given ip at the MTD of 30 mg/kg/day. Both compound **2** and compound **11** showed a highly significant inhibition of tumor growth throughout the study. The efficacy of the BIR3 ligands was similar to paclitaxel during the dosing period, but tumor growth resumed after cessation of therapy. A repeat study with compounds **2** and **11** showed similar results.

which is consistent with the potency of this caspase inhibitor in other cellular models of apoptosis.[23] Taken together, these results provide further evidence for mechanism-specific cell killing by active BIR3 ligands in susceptible human cancer cell lines.

In Vivo Efficacy of XIAP−BIR3 Ligands in the MDA-MB-231 Flank Breast Cancer Xenograft Model. We sought to investigate the efficacy of the potent BIR3 ligands **2** and **11** in the MDA-MB-231 flank breast cancer xenograft model. This model was chosen due to the remarkable in vitro sensitivity of this cell line to these compounds (EC_{50} = 0.068 and 0.013 μM for **2** and **11**, respectively, Table 5). As a negative control, the inactive *N*,*N*-dimethyl-Ala analogue **13** ($EC_{50} \geq 28$ μM) was also analyzed. The BIR3 ligands **2** and **11** showed significant efficacy in the MDA-MB-231 model (Figure 4). Consistent with in vitro analyses, compound **11** appeared slightly more potent in vivo than compound **2**. Compound **2** given at 40 mg/kg/day and compound **11** given at 20 mg/kg/day (near their maximum tolerated dose based on skin toxicity) each inhibited the tumor growth rate by 50−60% relative to the vehicle control. During the dosing period (day 14−30) tumor growth was essentially flat, and efficacy was

comparable to that observed for paclitaxel. However, unlike with paclitaxel treatment, tumor growth after termination of therapy resumed at a rate comparable to the vehicle control. Although the negative control compound **13** did show a modest separation from the vehicle control, the effect was transient and significantly less robust than that observed for the potent BIR3 ligands.

Conclusion

Starting from a micromolar natural peptide lead, a series of capped tripeptides was designed that contain unnatural amino acids and bind to the BIR3 domain of XIAP with single-digit nanomolar affinity. The proapoptotic activity of these compounds was demonstrated in an in vitro system that reconstitutes the cell's apoptotic machinery. Furthermore, these compounds exhibited remarkable cytotoxic activity in several cancer cell lines. Cytotoxic activity in the MDA-MB-231 breast cancer cell line translated into efficacy in the corresponding mouse xenograft model. The present study suggests that the BIR3 domain of XIAP represents a promising target for the development of small molecules that antagonize XIAP function and induce apoptosis.

Experimental Section

General. ^{1}H NMR spectra were obtained at 300 or 500 MHz using tetramethylsilane as the internal standard. For all proline-containing analogues two sets of signals originating from the two conformers were observed (ratio 9:1 to 3:1); the signal set for the major conformer is reported. Mass spectra (electron spray ionization mode) were recorded on Finnigan API SSQ7000 instruments. High-resolution mass spectra (fast atom bombardment mode) were recorded on a JEOL SX102A instrument. Flash chromatography was carried out on RediSep silicagel cartridges (ISCO) using an ISCO SQ100c chromatography station. Reactions were routinely conducted under nitrogen using commercial high purity solvents as received. Amino acid derivatives were purchased from Bachem, Fluka or NovaBiochem. Unless indicated otherwise, amino acids have the L-configuration. (4*S*)-Boc-4-phenoxy-Pro-OH was synthesized according to a literature reference.[20] LC/MS analysis was performed with a Phenomenex Luna C8 column (2.1 × 30 mm). TFA+ method: Gradient from 10 to 100% acetonitrile in 0.1% aqueous TFA (over 3.1 min; flow rate = 1.5 mL/min); AA+ method: As before, except 10 mM aqueous ammonium acetate instead of 0.1% aqueous TFA; MS data were aquired with APCI, positive ionization; UV detection at 220 nM. Preparative reversed phase HPLC was performed on a Waters Nova-Pak HR C18 6μm 60Å column (25 × 100 mm) using a gradient of 10 to 100% acetonitrile in 0.1% aqueous TFA (over 8 min; flow rate = 40 mL/min). Abbreviations: Cyclohexyl-glycine (Chg), 1,2-dichloroethane (DCE), *N*,*N*-dimethylacetamide (DMA), *N*,*N*-diisopropylethylamine (DIPEA), 1-ethyl-3-(3-dimethylaminopropyl)carbodiimide (EDCI), 1-hydroxy-7-azabenzotriazole (HOAt), 1-hydroxybenzotriazole (HOBt), trifluoroacetic acid (TFA), triisopropylsilane (TIS), *tert*-leucine/*tert*-butylglycine (Tle).

Parallel Synthesis of Peptide Libraries. The chambers of a Robbins reaction block (Robbins Scientific) were filled with 50 μmol of Rink MBHA resin (Novabiochem) carrying the following amino acid sequences: Position 1 library: Fmoc-Val-Pro-Phe-Tyr(^{t}Bu)-NH-resin; position 2 library: Fmoc-Pro-Phe-Tyr(^{t}Bu)-NH-resin; position 3 library: Fmoc-Phe-Tyr(^{t}Bu)-NH-resin; position 4 library: Fmoc-Tyr(^{t}Bu)-NH-resin.

Removal of Fmoc group: The resins in each chamber were treated twice with 4 mL of 20% piperidine in DMF (3 min each cycle). After filtration, all resins were washed three times with 4 mL of DMF. Amino acid activation: The Fmoc-protected amino acids (500 μmol) were each dissolved in 2 mL of a 0.25 M solution of HOAt (500 μmol) in DMF. *N*,*N*′-diisopropylcarbodiimide (79 μL, 500 μmol each) was added, and the solutions were allowed to stand for 5 min before coupling. If a position of the pentapeptide was not varied, a stock solution (100 mL) of the respective amino acid (Ala, Val, or Pro) was prepared.

Coupling: Solutions of the activated amino acids (2 mL) were added to the respective chambers in the Robbins block and the block was agitated for 1 h. After filtration, the resins were washed three times with 4 mL of DMF. The deprotection/coupling cycle was repeated until the pentapeptide stage. Each resin was washed twice with 4 mL of DMF, MeOH, and diethyl ether. To cleave the pentapeptides and remove the side chain protecting groups, 1 mL of a TFA/H_2O/TIS cocktail (95:2.5:2.5) was added to each chamber containing the air-dry resins and the block was agitated for 1 h. The peptide solutions were filtered into a Robbins collection block and the resins were washed twice with TFA. After drying the sample in a Genevac HT4 evaporator, the remaining residues were dissolved in water/MeOH (1:1) and purified by preparative RP-HPLC. The pentapeptides were isolated as TFA salts in >95% purity (LC/MS and ^{1}H NMR analysis).

General Procedure for Solution-Phase Peptide Coupling. EDCI (6.33 g, 33.0 mmol) was added to a stirred solution of the Boc-protected amino acid (30.0 mmol), DIPEA (5.23 mL, 30.0 mmol), and HOBt (4.46 g, 33.0 mmol) in DMF (50 mL) at 0 °C. If the amine coupling partner was used as the HCl salt, the amount of DIPEA was doubled. After 5 min, the amino component (33.0 mmol) was added to the ice-cold coupling solution, and the reaction was stirred overnight at room temp. The mixture was diluted with EtOAc and washed twice with 1 N aqueous HCl, $NaHCO_3$ solution and brine, respectively. The organic layer was dried over $MgSO_4$, and the volatiles were removed under reduced pressure. The coupling product was purified by flash chromatography (gradient of EtOAc in hexane).

General Procedure for Removal of the Boc Protecting Group. The Boc-protected compound (30 mmol) was stirred with 4 N HCl in dioxane (50 mL) for 1 h at room temp. The volatiles were removed under reduced pressure, and the residue was coevaporated twice with diethyl ether. The HCl salt was dried in vacuo.

Synthesis of Capped Tripeptide Library. Boc−*N*-Me-Ala-Tle-Pro-OH (1). Utilizing the general procedures for peptide coupling and Boc removal, the benzyl-protected tripeptide Boc-*N*-Me-Ala-Tle-Pro-OBn was synthesized (H-Pro-OBn HCl salt, Boc-Tle-OH, Boc-*N*-Me-Ala as the coupling components). To a solution of the benzyl ester (2.35 g, 4.67 mmol) in MeOH (50 mL) was added palladium on charcoal (5%, 100 mg), and the reaction was stirred under a hydrogen atmosphere for 18 h. The catalyst was filtered off over Celite, and the filtrate was concentrated under reduced pressure to yield 1.76 g of a white foam (92%). ^{1}H NMR (500 MHz, MeOH-d_4) δ 4.61 (m, 2H), 4.41 (dd, 1H), 3.87 (m, 1H), 3.73 (m, 1H), 2.85 (s, 3H), 2.27 (m, 1H), 1.95−2.10 (m, 3H), 1.47 (s, 9H), 1.33 (d, 3H), 1.05 (s, 9H). MS m/z = 414 $(M+H)^+$, 436 $(M+Na)^+$.

Coupling of Tripeptide Acid 1 with Amino Caps. The chambers of a Robbins reaction block were filled with PS-Carbodiimide resin (Argonaut Technologies, 70 mg, f = 2 mmol/g, 140 μmol). To each chamber was added a solution of the respective amine (70 μmol, 0.35 mL of a 0.2 M solution in DMA), a solution of the tripeptide acid **1** (85 μmol, 0.85 mL of a 0.1 M solution in 20% DMA in DCE), and a solution of HOAt (120 μmol, 0.6 mL of 0.2 M solution in 20% DMA in DCE). The reaction block was shaken for 18 h at room temp. To scavenge excess acid, PS-Trisamine resin (Argonaut Technologies, 70 mg, f = 3 mmol/g, 210 μmol) was added to each reaction chamber, and the block was agitated for an additional 3 h. Then, the reaction solutions were filtered into a Robbins collection block and the volatiles were removed in a Genevac HT4 evaporator. To remove the N-terminal Boc-group, the residue in each chamber was treated with 1 mL of a TFA/H_2O/TIS cocktail (95:2.5:2.5) for 1 h. After drying the sample in the evaporator, the remaing residues were dissolved in water/MeOH (1:1) and purified by preparative RP-HPLC. The capped

Table 6

compd	first amino acid	second amino acid	third amino acid
2	Boc-*N*-Me-Ala-OH	Boc-Tle-OH	Boc-Pro-OH
10	Boc-*N*-Me-Ala-OH	Boc-Tle-OH	(4*S*)-Boc-4-phenoxy-Pro-OH
11	Boc-*N*-Me-Ala-OH	Boc-Chg-OH	Boc-Pro-OH
12	Boc-*N*-Me-Ala-OH	Boc-Chg-OH	(4*S*)-Boc-4-phenoxy-Pro-OH
13	*N*,*N*-Me$_2$-Ala-OH	Boc-Tle-OH	Boc-Pro-OH
14	*N*,*N*-Me$_2$-Ala-OH	Boc-Tle-OH	(4*S*)-Boc-4-phenoxy-Pro-OH
15	*N*,*N*-Me$_2$-Ala-OH	Boc-Chg-OH	Boc-Pro-OH
16	Boc-*N*-Me-D-Ala-OH	Boc-Tle-OH	Boc-Pro-OH

tripeptides were isolated as the TFA salts in 50−80% yield and >95% purity (LC/MS analysis).

H-*N*-Me-Ala-Tle-Pro-(*R*)-tetrahydronaphth-1-yl Amide (2). t_R (TFA+) = 1.47 min; t_R (AA+) = 1.55 min. ^{1}H NMR (500 MHz, D_2O) δ 7.19−7.35 (m, 4H), 4.99 (m, 1H), 4.64 (s, 1H), 4.39 (m, 1H), 4.07 (m, 1H), 3.95 (m, 1H), 3.77 (m, 1H), 2.80 (m, 2H), 2.71 (s, 3H), 2.30 (m, 1H), 1.77−2.17 (m, 7H), 1.50 (d, 3H), 1.10 (s, 9H). MS m/z = 443 $(M+H)^+$. HRMS for $[C_{25}H_{39}N_4O_3]^+$ 443.3022; found 443.3015.

H-*N*-Me-Ala-Tle-Pro-(*S*)-tetrahydronaphth-1-yl Amide (3). t_R (TFA+) = 1.49 min; t_R (AA+) = 1.56 min. ^{1}H NMR (500 MHz, MeOH-d_4) δ 7.05−7.17 (m, 4H), 5.02 (t, 1H), 4.63 (s, 1H), 4.38 (m, 1H), 3.93 (m, 2H), 3.74 (m, 1H), 2.70−2.85 (m, 2H), 2.66 (s, 3H), 1.75−2.23 (m, 8H), 1.45 (d, 3H), 1.10 (s, 9H). MS m/z = 443 $(M+H)^+$.

H-*N*-Me-Ala-Tle-Pro-(*R*)-indan-1-yl Amide (4). t_R (TFA+) = 1.41 min; t_R (AA+) = 1.47 min. ^{1}H NMR (500 MHz, MeOH-d_4) δ 7.40 (d, 1H), 7.10−7.25 (m, 3H), 5.35 (t, 1H), 4.66 (s, 1H), 4.38 (m, 1H), 3.93 (m, 2H), 3.75 (m, 1H), 2.98 (m, 1H), 2.87 (m, 1H), 2.66 (s, 3H), 2.47 (m, 1H), 2.10−2.25 (m, 2H), 1.80−2.02 (m, 3H), 1.46 (d, 3H), 1.13 (s, 9H). MS m/z =429 $(M+H)^+$. HRMS for $[C_{24}H_{37}N_4O_3]^+$ 429.2866; found 429.2868.

H-*N*-Me-Ala-Tle-Pro-(*S*)-indan-1-yl Amide (5). t_R (TFA+) = 1.42 min; t_R (AA+) = 1.47 min. ^{1}H NMR (500 MHz, MeOH-d_4) δ 7.20 (m, 4H), 5.33 (t, 1H), 4.64 (s, 1H), 4.40 (m, 1H), 3.93 (m, 2H), 3.75 (m, 1H), 3.00 (m, 1H), 2.86 (m, 1H), 2.66 (s, 3H), 2.50 (m, 1H), 1.87−2.25 (m, 5H), 1.46 (d, 3H), 1.10 (s, 9H). MS m/z = 429 $(M+H)^+$.

H-*N*-Me-Ala-Tle-Pro-naphth-1-yl Amide (6). t_R (TFA+) = 1.47 min; t_R (AA+) = 1.55 min. ^{1}H NMR (500 MHz, MeOH-d_4) δ 8.15 (m, 1H), 7.89 (m, 1H), 7.78 (m, 1H), 7.45−7.58 (m, 4H), 4.75 (m, 1H), 4.69 (s, 1H), 3.99 (m, 2H), 3.78 (m, 1H), 2.68 (s, 3H), 2.40 (m, 1H), 2.20 (m, 2H), 2.03 (m, 1H), 1.52 (d, 3H), 1.10 (s, 9H). MS m/z = 439 $(M+H)^+$.

H-*N*-Me-Ala-Tle-Pro-naphth-2-yl Amide (7). t_R (TFA+) = 1.62 min; t_R (AA+) = 1.71 min. ^{1}H NMR (500 MHz, MeOH-d_4) δ 8.20 (m, 1H), 7.77 (m, 3H), 7.54 (dd, 1H), 7.35−7.47 (m, 2H), 4.69 (s, 1H), 4.59 (m, 1H), 3.96 (m, 2H), 3.80 (m, 1H), 2.67 (s, 3H), 2.33 (m, 1H), 1.95−2.21 (m, 3H), 1.48 (d, 3H), 1.13 (s, 9H). MS m/z = 439 $(M+H)^+$.

H-*N*-Me-Ala-Tle-Pro-fluoren-9-yl Amide (8). t_R (TFA+) = 1.62 min; t_R (AA+) = 1.73 min. ^{1}H NMR (500 MHz, MeOH-d_4) δ 7.05−7.60 (m, 8H), 5.90 (s, 1H), 4.53 (s, 1H), 4.27 (t, 1H), 3.80 (m, 2H), 3.65 (m, 1H), 2.58 (s, 3H), 1.83−2.30 (m, 4H), 1.42 (d, 3H), 1.12 (s, 9H). MS m/z = 477 $(M+H)^+$.

H-*N*-Me-Ala-Tle-Pro-phenethyl Amide (9). t_R (TFA+) = 1.42 min; t_R (AA+) = 0.97 min. ^{1}H NMR (300 MHz, MeOH-d_4) δ 7.15−7.32 (m, 5H), 4.63 (m, 1H), 4.32 (m, 1H), 3.90 (m, 2H), 3.70 (m, 1H), 3.34−3.55 (m, 2H), 2.80 (m, 2H), 2.66 (s, 3H), 1.75−2.15 (m, 4H), 1.46 (d, 3H), 1.09 (s, 9H). MS m/z = 417 $(M+H)^+$.

H-*N*-Me-Ala-Tle-Pro-(*R*)-tetrahydronaphth-1-yl Amide (2) was resynthesized in 12 mmol scale utilizing the standard procedures for peptide coupling and Boc-removal to provide 4.97 g of the final product as the HCl salt (87% yield; (*R*)-1-amino-1,2,3,4-tetrahydronaphthalene, Boc-Tle-OH, Boc-*N*-Me-Ala as the coupling components). Compounds **10**−**16** were synthesized analogously to compound **2** using the building blocks shown in the Table 6.

H-*N*-Me-Ala-Tle-(4*S*)-4-phenoxy-Pro-(*R*)-tetrahydronaphth-1-yl Amide (10). t_R (TFA+) = 1.78 min; t_R (AA+) = 1.93 min. ^{1}H NMR (500 MHz, D_2O) δ 7.05−7.35 (m, 6H), 6.67−7.00 (m, 3H), 5.11 (m, 1H), 4.93 (m, 1H), 4.57 (m, 1H), 4.44 (s, 1H), 3.83−4.05 (m, 3H), 2.52−2.75 (m, 6H), 2.38 (m, 1H), 1.55−1.85 (m, 3H), 1.39−1.50 (m, 4H), 0.87 (s, 9H). MS m/z = 535 $(M+H)^+$. HRMS for $[C_{31}H_{43}N_4O_4]^+$ 535.3284; found 535.3279.

H-*N*-Me-Ala-Chg-Pro-(*R*)-tetrahydronaphth-1-yl Amide (11). t_R (TFA+) = 1.58 min; t_R (AA+) = 1.66 min. ^{1}H NMR (500 MHz, D_2O) δ 7.13−7.25 (m, 4H), 4.96 (m, 1H), 4.55 (d, 1H), 4.35 (m, 1H), 3.98 (m, 1H), 3.87 (m, 1H), 3.73 (m, 1H), 2.77 (m, 2H), 2.70 (s, 3H), 2.30 (m, 1H), 1.93−2.13 (m, 4H), 1.57−1.90 (m, 9H), 1.50 (d, 3H), 1.05−1.30 (m, 5H). MS m/z = 469 $(M+H)^+$. HRMS for $[C_{27}H_{41}N_4O_3]^+$ 469.3179; found 469.3185.

H-*N*-Me-Ala-Chg-(4*S*)-4-phenoxy-Pro-(*R*)-tetrahydronaphth-1-yl Amide (12). t_R (TFA+) = 1.83 min; t_R (AA+) = 2.05 min. ^{1}H NMR (500 MHz, D_2O) δ 6.53−7.30 (m, 9H), 5.09 (m, 1H), 4.92 (m, 1H), 4.51 (d, 1H), 4.30 (d, 1H), 3.84−3.98 (m, 3H), 2.54−2.73 (m, 6H), 2.38 (d, 1H), 1.33−1.87 (m, 13H), 0.72−1.02 (m, 5H). MS m/z = 561 $(M+H)^+$. HRMS for $[C_{33}H_{45}N_4O_4]^+$ 561.3441; found 561.3441.

H-*N*,*N*-Me$_2$-Ala-Tle-Pro-(*R*)-tetrahydronaphth-1-yl Amide (13). t_R (TFA+) = 1.46 min; t_R (AA+) = 1.85 min. ^{1}H NMR (500 MHz, D_2O) δ 7.19−7.34 (m, 4H), 4.99 (t, 1H), 4.64 (s, 1H), 4.40 (m, 1H), 4.10 (m, 1H), 3.95 (m, 1H), 3.76 (m, 1H), 2.92 (s, 6H), 2.80 (m, 2H), 2.31 (m, 1H), 2.12 (m, 1H), 1.73−2.05 (m, 6H), 1.54 (d, 3H), 1.10 (s, 9H). MS m/z = 457 $(M+H)^+$. HRMS for $[C_{26}H_{41}N_4O_3]^+$ 457.3179; found 457.3182.

H-*N*,*N*-Me$_2$-Ala-Tle-(4*S*)-4-phenoxy-Pro-(*R*)-tetrahydronaphth-1-yl Amide (14). t_R (TFA+) = 1.80 min; t_R (AA+) = 2.23 min. ^{1}H NMR (300 MHz, DMSO-d_6) δ 9.75 (br s, 1H), 8.76 (d, 1H), 8.11 (d, 1H), 6.82−7.35 (m, 10H), 5.06 (m, 1H), 4.95 (m, 1H), 4.48 (m, 2H), 4.23 (m, 1H), 4.05 (m, 1H), 3.68 (m, 1H), 2.52−2.82 (m, 9H), 1.55−2.10 (m, 4H), 1.37 (d, 3H), 1.02 (s, 9H). MS m/z = 549 $(M+H)^+$. HRMS for $[C_{32}H_{45}N_4O_4]^+$ 549.3441; found 549.3455.

H-*N*,*N*-Me$_2$-Ala-Chg-Pro-(*R*)-tetrahydronaphth-1-yl Amide (15). t_R (TFA+) = 1.57 min; t_R (AA+) = 1.96 min. ^{1}H NMR (500 MHz, D_2O) δ 7.19−7.31 (m, 4H), 4.99 (t, 1H), 4.57 (d, 1H), 4.39 (m, 1H), 4.04 (m, 1H), 3.91 (m, 1H), 3.75 (m, 1H), 2.91 (s, 6H), 2.80 (m, 2H), 2.31 (m, 1H), 1.62−2.15 (m, 13H), 1.54 (d, 3H), 1.05−1.30 (m, 5H). MS m/z = 483 $(M+H)^+$. HRMS for $[C_{28}H_{43}N_4O_3]^+$ 483.3335; found 483.3350.

H−*N*-Me-D-Ala-Tle-Pro-(*R*)-tetrahydronaphth-1-yl Amide (16). t_R (TFA+) = 1.45 min; t_R (AA+) = 1.56 min. ^{1}H NMR (300 MHz, D_2O) δ 7.17−7.35 (m, 4H), 4.99 (m, 1H), 4.61 (s, 1H), 4.39 (m, 1H), 3.70−4.09 (m, 3H), 2.80 (m, 2H), 2.67 (s, 3H), 2.30 (m, 1H), 1.72−2.15 (m, 7H), 1.57 (d, 3H), 1.08 (s, 9H). MS m/z = 443 $(M+H)^+$. HRMS for $[C_{25}H_{39}N_4O_3]^+$ 443.3022; found 443.3040.

Expression and Purification of BIR3 Protein. The BIR3 protein was prepared as described.[24] NMR samples contained 0.8 mM protein in either 90% H_2O/10% ^2H_2O or 100% ^2H_2O, 10 mM phosphate (pH 7.2), 120 mM NaCl, and 2 mM ^{2}H-dithiothreitol.

NMR Spectroscopy. All NMR experiments were acquired at 303 K on a Bruker DRX600 NMR spectrometer. Resonances were assigned using both nuclear Overhauser enhancement spectroscopy (NOESY) and total correlation spectroscopy (TOCSY) experiments.[25] The protein side chain ^{1}H and ^{13}C NMR signals were assigned from both HCCH-TOCSY experiments and 3D ^{13}C- or ^{15}N-edited NOESY experiments. Protein resonances assignments were made with the aid of our earlier assignments for the Bir3/Smac peptide complex.[11] Stereospecific assignments of the valine and leucine methyl groups were derived from our earlier Bir3/Smac peptide complex.[11] Ligand assignments and constraints were obtained from a 2D ^{13}C,^{15}N-filtered NOESY and 2D ^{13}C,^{15}N-filtered TOCSY experiment.[26,27] NOE distance restraints (protein−protein and protein−ligand) were obtained from three-dimensional ^{13}C-edited,^{15}N-edited, and ^{13}C,^{15}N-filtered ^{13}C-edited NOESY experiments[26,27] acquired with a mixing time of 80 ms.

Ligand−ligand constraints were obtained from the 2D $^{13}C,^{15}N$-filtered NOESY experiment with a mixing time of 100 ms.

Structure Calculations. BIR3/ligand structures were calculated using a docking protocol implemented with the program Xplor-NIH.[28,29] Ligands were docked into the previously determined BIR3/SMAC average structure using rigid body docking of the ligand and the protein followed by energy minimization of the protein and ligand structures to optimize the conformation of the complex. In the final refinement stage, the protein and ligand conformation were refined based on the NMR derived constraints. A square-well potential (FNOE = 50 kcal mol^{-1}) was employed to constrain NOE-derived distances. On the basis of the cross-peak intensities, NOE-derived distance restraints for the protein were given upper bounds of 3.0, 4.0, or 5.0 Å, while the intermolecular distance restraints were given upper bounds of 3.5 or 5.0 Å. Eight/ten intraligand NOES and 95/108 intermolecular NOEs were obtained for ligand **2**/**10**, respectively. Protein−protein NOE restraints were reassigned and quantitated for protein residues in the vicinity of the ligand resulting in 39/41 constraints for ligand **2**/**10**, respectively. Restraints for the remainder of the protein were derived from our earlier BIR3/SMAC peptide structure. This resulted in an additional 477 unambiguous protein−protein NOE restraints, 36 hydrogen-bond restraints, and 86 ϕ and φ angular restraints derived from the Talos program that were used in the docking calculations. Superposition of the protein backbone for the 10 lowest energy structures resulted in an rmsd of 0.10, 0.08 Å for the heavy atoms of ligands **2** and **10**, respectively.

Ligand Binding. A fluorescence polarization anisotropy (FPA) competition assay was used to determine the affinities of compounds to BIR3 protein.[11] Fluorescence polarization measurements were carried out on an Analyst 96-well plate reader (LJL, Molecular Dynamic, Sunnyvale, CA). 6-Carboxyfluorescein (FAM) labeled peptides with the sequences AVPIAQK(FAM)-NH_2 and AVPFAAK(FAM)-NH_2 were used as probes. To measure the potent compounds more accurately, a tight-binding probe was designed and synthesized by substituting the position 2 residue Tle of compound **10** with a Lys residue that bears a FAM label at the ϵ-amino group. This probe binds to the BIR3 protein with K_d of 7 nM. Dissociation constants were determined from titration curves with in-house written software using the analytical expressions of Wang.[30]

Reconstituted Caspase Activation Assays. Apaf-1 (4.0 nM), Csp-9 (p35/p12) or procaspase-9 (4.0 nM), 60 ng of procsp-3, 200 μM dATP and 600 nM cytochrome C were preincubated with 100 nM BIR3 or 5 nM XIAP in a final volume of 20 μL at 30 °C for 30 min. Increasing amounts of compound or SMAC were then added to a final volume of 40 μL. Following incubation for 30 min at 30 °C, DEVDamc cleavage activity was assessed. Activity is expressed as an EC_{50}, the concentration at which half-maximum recovery was achieved.

Cell Viability. Human cancer cell lines were cultured in suitable culture media containing 10% FBS. Adherent cell lines were plated in 96-well plates and allowed to adhere for 24 to 48 h prior to compound exposure. Suspension cell lines were used without preincubation. Cells were exposed to various concentrations of compound for 48 or 72 h, and viability was measured by MTS reduction with a commercial kit (Promega, Madison, WI, CellTiter 96 Aqueous Assay). To assess protection from BIR3 ligand toxicity by the pan-caspase inhibitor IDN-5370, cells were exposed for 48 h to 10 μM BIR3 ligand and various concentrations of IDN5370, followed by measuring viability.

Caspase-3 Activity. Cells were lysed on ice in 0.1% Triton X-100, 10 mM Hepes, 42 mM KCl, 5 mM $MgCl_2$, pH 7.4, 1 mM DTT, and protease inhibitors (BD Biosciences, Franklin Lakes, NJ, Cat #554779) after compound exposure and caspase-3 activity was measured in 20 mM Hepes, 1 mM EDTA, 0.1% CHAPS, 10% sucrose, 10 mM DTT, pH 7.5 with 20 μM Ac-DEVD-amc as substrate by following the release of aminomethylcoumarin.

Xenograft Efficacy Studies. MDA-MB-231 cells were obtained from the American Type Culture Collection (Manassas, VA) and were grown to passage 3 prior to inoculation. The cells were mixed with Matrigel (BD Biosciences, Bedford, MA) at a 1:1 ratio and 5×10^6 cells were inoculated into the right flank of female scid mice (C.B-17-*Prkdc*^{scid}, Charles River Laboratories, Wilmington, MA). Tumors were measured by digital calipers and the formula $V = LW^2/2$ was used to estimate tumor size. Thirteen days after inoculation, mice were assigned to treatment groups ($N = 10$ per group) with an average volume of approximately 230 mm^3 per group. Tumor size was then monitored by twice weekly measurements. The Wilcoxon Rank Sum test was used to compare tumor size between groups. The BIR3 ligands were both formulated in 0.1 M PBS, pH 5−6.

Acknowledgment. The authors would like to thank Jennifer Bouska, Paul Richardson, and Xenia Searle for technical assistance. We also thank the Abbott High-Throughput Purification group and the Structural Chemistry group.

Supporting Information Available: Stereoviews of NMR-derived structures of compounds **2**, **10**, and AVPI bound to the BIR3 domain of XIAP; BIR3 binding data for compounds from the first library; toxicity of BIR3 ligands against 59 human cancer cell lines. This material is available free of charge via the Internet at http://pubs.acs.org.

References

(1) Deveraux, Q. L.; Reed, J. C. IAP family proteins-suppressors of apoptosis. *Genes Dev.* **1999**, *13*, 239−252.
(2) Tamm, I.; Kornblau, S. M.; Segall, H.; Krajewski, S.; Welsh, K.; Kitada, S.; Scudiero, D. A.; Tudor, G.; Qui, Y. H.; Monks, A.; Andreeff, M.; Reed, J. C. Expression and prognostic significance of IAP-family genes in human cancers and myeloid leukemias. *Clin. Cancer Res.* **2000**, *6*, 1796−1803.
(3) Krajewska, M.; Krajewski, S.; Banares, S.; Huang, X.; Turner, B.; Bubendorf, L.; Kallioniemi, O. P.; Shabaik, A.; Vitiello, A.; Peehl, D.; Gao, G. J.; Reed, J. C. Elevated expression of inhibitor of apoptosis proteins in prostate cancer. *Clin. Cancer Res.* **2003**, *9*, 4914−4925.
(4) Srinivasula, S. M.; Hegde, R.; Saleh, A.; Datta, P.; Shiozaki, E.; Chai, J.; Lee, R. A.; Robbins, P. D.; Fernandes-Alnemri, T.; Shi, Y.; Alnemri, E. S. A conserved XIAP-interaction motif in caspase-9 and Smac/DIABLO regulates caspase activity and apoptosis. *Nature* **2001**, *410*, 112−116.
(5) Shiozaki, E. N.; Chai, J.; Rigotti, D. J.; Riedl, S. J.; Li, P.; Srinivasula, S. M.; Alnemri, E. S.; Fairman, R.; Shi, Y. Mechanism of XIAP-mediated inhibition of caspase-9. *Mol. Cell* **2003**, *11*, 519−527.
(6) Chai, J.; Shiozaki, E.; Srinivasula, S. M.; Wu, Q.; Datta, P.; Alnemri, E. S.; Shi, Y.; Dataa, P. Structural basis of caspase-7 inhibition by XIAP. *Cell* **2001**, *104*, 769−780.
(7) Huang, Y.; Park, Y.; Rich, R. L.; Segal, D.; Myszka, D. G.; Wu, H. Structural basis of caspase inhibition by XIAP: differential roles of the linker versus the BIR domain. *Cell* **2001**, *104*, 781−790.
(8) Riedl, S. J.; Renatus, M.; Schwarzenbacher, R.; Zhou, Q.; Sun, C.; Fesik, S. W.; Liddington, R. C.; Salvesen, G. S. Structural basis for the inhibition of caspase-3 by XIAP. *Cell* **2001**, *104*, 791−800.
(9) Du, C.; Fang, M.; Li, Y.; Li, L.; Wang, X. Smac, a mitochondrial protein that promotes cytochrome *c*-dependent caspase activation by eliminating IAP inhibition. *Cell* **2000** *102*, 33−42.
(10) Verhagen, A. M.; Ekert, P. G.; Pakusch, M.; Silke, J.; Connolly, L. M.; Reid, G. E.; Moritz, R. L.; Simpson, R. J.; Vaux, D. L. Identification of DIABLO, a mammalian protein that promotes apoptosis by binding to and antagonizing IAP proteins. *Cell* **2000**, *102*, 43−53.
(11) Liu, Z.; Sun, C.; Olejniczak, E. T.; Meadows, R. P.; Betz, S. F.; Oost, T.; Herrmann, J.; Wu, J. C.; Fesik, S. W. Structural basis for binding of Smac/DIABLO to the XIAP BIR3 domain. *Nature* **2000**, *408*, 1004−1008.
(12) Wu, G.; Chai, J.; Suber, T. L.; Wu, J. W.; Du, C.; Wang, X.; Shi Y. Structural basis of IAP recognition by Smac/DIABLO. *Nature* **2000**, *408*, 1008−1012.
(13) Chai, J.; Du, C.; Wu, J.-W.; Kyin, S.; Wang, X.; Shi, Y. Structural and biochemical basis of apoptotic activation by Smac/DIABLO. *Nature* **2000**, *406*, 855−862.
(14) Arnt, C. R.; Chiorean, M. V.; Heldebrant M. P.; Gores G. J.; Kaufmann, S. H. Synthetic Smac/DIABLO peptides enhance the effects of chemotherapeutic agents by binding XIAP and cIAP1 in situ. *J. Biol. Chem.* **2002**, *277*, 44236−44243.

(15) Guo, F.; Nimmanapalli, R.; Paranawithana, S.; Wittman, S.; Griffin, D.; Bali, P.; O'Bryan, E.; Fumero, C.; Wang, H. G.; Bhalla, K. Ectopic overexpression of second mitochondria-derived activator of caspases (Smac/DIABLO) or cotreatment with N-terminus of Smac/DIABLO peptide potentiates epothilone B derivative-(BMS 247550) and Apo-2L/TRAIL-induced apoptosis. *Blood* **2002**, *99*, 3419−3426.
(16) Yang, L.; Mashima, T.; Sato, S.; Mochizuki, M.; Sakamoto, H.; Yamori, T.; Oh-Hara, T.; Tsuruo, T. Predominant suppression of apoptosome by inhibitor of apoptosis protein in nonsmall cell lung cancer H460 cells: therapeutic effect of a novel polyarginine-conjugated Smac peptide. *Cancer Res.* **2003**, *15*, 831−837.
(17) Fulda, S.; Wick, W.; Weller, M.; Debatin, K.-M. Smac agonists sensitize for Apo2L/TRAIL- or anticancer drug-induced apoptosis and induce regression of malignant glioma in vivo. *Nat. Med.* **2002**, *8*, 808−815.
(18) Vucic, D.; Kaiser, W. J.; Miller, L. K. Inhibitor of apoptosis proteins physically interact with and block apoptosis induced by *Drosophila* proteins Hid and Grim. *Mol. Cell Biol.* **1998**, *18*, 3300−3309.
(19) Kipp, R. A.; Case, M. A.; Wist, A. D.; Cresson, C. M.; Carrell, M.; Griner, E.; Wiita, A.; Albiniak, P. A.; Chai, J.; Shi, Y.; Semmelhack, M. F.; McLendon, G. L. Molecular targeting of inhibitor of apoptosis proteins based on small molecule mimics of natural binding partners. *Biochemistry* **2002**, *41*, 7344−7349.
(20) Bellier, B.; McCort-Tranchepain, I.; Ducos, B.; Danascimento, S.; Meudal, H.; Noble, F.; Garbay, C.; Roques, B. P. Synthesis and Biological Properties of New Constrained CCK-B Antagonists: Discrimination of Two Affinity States of the CCK-B Receptor on Transfected CHO Cells. *J. Med. Chem.* **1997**, *40*, 3947−3956.
(21) Zou, H.; Yang, R.; Hao, J.; Wang, J.; Sun, C.; Fesik, S. W.; Wu, J. C.; Tomaselli, K. J.; Armstrong, R. C. Regulation of the Apaf-1/caspase-9 apoptosome by caspase-3 and XIAP. *J. Biol. Chem.* **2003**, *278*, 8091−8098.
(22) Huang, Y.; Rich R. L.; Myszka, D. G.; Wu, H. Requirement of both the second and third BIR domains for the relief of X-linked inhibitor of apoptosis protein (XIAP)-mediated caspase inhibition by Smac. *J. Biol. Chem.* **2003**, *278*, 49517−49522.
(23) Deckwerth, T. L. et al. Long-term protection of brain tissue from cerebral ischemia by peripherally administered peptidomimetic caspase Inhibitors. *Drug Dev. Res.* **2001**, *52*, 579−586.
(24) Sun, C.; Cai, M.; Meadows, R. P.; Xu, N.; Gunasekera, A. H.; Herrmann, J.; Wu, J. C.; Fesik, S. W. NMR structure and mutagenesis of the third Bir domain of the inhibitor of apoptosis protein XIAP. *J. Biol. Chem.* **2000**, *275*, 33777−33781.
(25) Clore, G. M.; Gronenborn, A. M. Multidimensional heteronuclear nuclear magnetic resonance of proteins. *Methods Enzymol.* **1994**, *239*, 349−363.
(26) Fesik, S. W.; Zuiderweg, E. R. P. *J. Magn. Reson.* **1988**, *78*, 588−593.
(27) Marion, D.; Driscoll, P. C.; Kay, L. E.; Wingfield, P. T.; Bax, A.; Gronenborn, A. M.; Clore, G. M. Overcoming the overlap problem in the assignment of 1H NMR spectra of larger proteins by use of three-dimensional heteronuclear ^{1}H-^{15}N Hartmann−Hahn-multiple quantum coherence and nuclear Overhauser-multiple quantum coherence spectroscopy: application to interleukin 1 beta. *Biochemistry* **1989**, *29*, 6150−6156.
(28) Brunger, A. T. X-PLOR Version 3.1, Yale University Press, New Haven and London, 1992.
(29) Schwieters, C. D.; Kuszewski, J. J.; Tjandra, N.; Clore, G. M. The Xplor-NIH NMR molecular structure determination package. *J. Magn. Reson.* **2003**, *160*, 65−73.
(30) Wang, Z.-X. An exact mathematical expression for describing competitive binding of two different ligands to a protein molecule. *FEBS Lett.* **1995**, *360*, 111−114.

JM040037K